Title: Using microfluidics for scalable manufacturing of nanomedicines from bench to GMP: A case study using protein-loaded liposomes.

Authors: Cameron Webb[1+], Neil Forbes[1+], Carla B. Roces[1], Giulia Anderluzzi[1], Gustavo Lou[1], Suraj Abraham[2], Logan Ingalls[2], Keara Marshall[2], Timothy J Leaver[2], Julie A Watts[3], Jonathan W Aylott[3] and Yvonne Perrie[1*]

[1]Strathclyde Institute of Pharmacy and Biomedical Sciences, University of Strathclyde, Glasgow, Scotland, UK. G4 0RE.

[2]Precision NanoSystems Inc, #50 655 W Kent Ave N, Vancouver, BC V6P 6T7

[3]School of Pharmacy, University of Nottingham, University Park, Nottingham, England, UK. NG7 2RD

[+]these authors contributed equally to this work

Key Words: microfluidics, manufacture, liposomes, nanomedicines, continuous, scale-independent.

***Corresponding author**:

Professor Yvonne Perrie
Strathclyde Institute of Pharmacy and Biomedical Sciences,
161 Cathedral St,
University of Strathclyde,
Glasgow, G4 0RE
Scotland.
yvonne.perrie@strath.ac.uk

Abstract

Nanomedicines are well recognised for their ability to improve therapeutic outcomes. Yet, due to their complexity, nanomedicines are challenging and costly to produce using traditional manufacturing methods. For nanomedicines to be widely exploited, new manufacturing technologies must be adopted to reduce development costs and provide a consistent product. Within this study, we investigate microfluidic manufacture of nanomedicines. Using protein-loaded liposomes as a case study, we manufacture liposomes with tightly defined physico-chemical attributes (size, PDI, protein loading and release) from small-scale (1 mL) through to GMP volume production (200 mL/min). To achieve this, we investigate two different laminar flow microfluidic cartridge designs (based on a staggered herringbone design and a novel toroidal mixer design); for the first time we demonstrate the use of a new microfluidic cartridge design which delivers seamless scale-up production from bench-scale (12 mL/min) through GMP production requirements of over 20 L/h using the same standardised normal operating parameters. We also outline the application of tangential flow filtration for down-stream processing and high product yield. This work confirms that defined liposome products can be manufactured rapidly and reproducibly using a scale-independent production process, thereby de-risking the journey from bench to approved product.

Graphical abstract

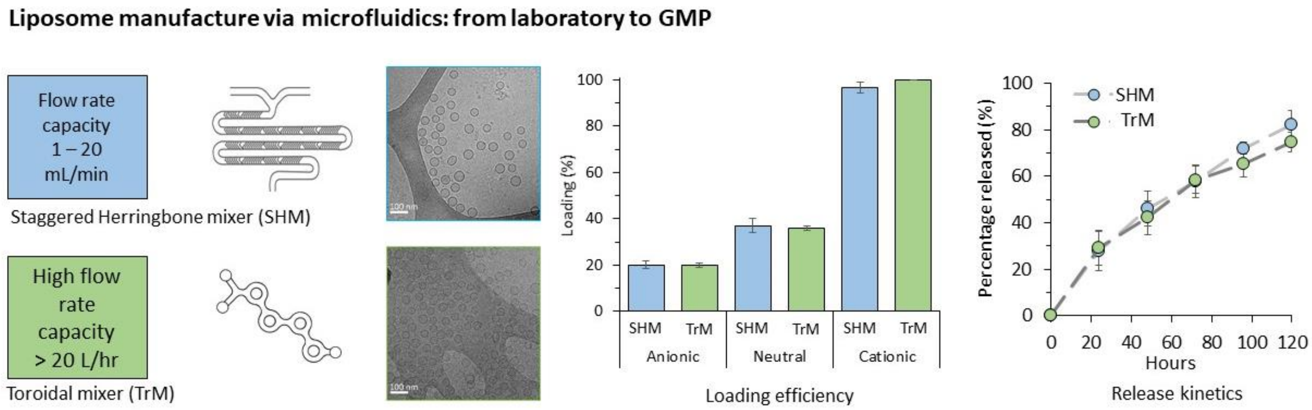

1. Introduction

Developments in nanomedicines continue to provide new advances in healthcare, with lipid-based formulations playing a central role. Since the first approved product, AmBisome® (Gilead), which was approved in 1990 in Europe (and subsequently in the USA in 1997), a range of liposomal nanomedicines have been approved (e.g. Doxil®/Caelyx®, DaunoXome®, Myocet®, Visudyne®, Marqibo®, Onivyde® and Vyxeos®). The majority of these products are used to improve drug delivery and reduce off-target toxicity associated with the incorporated cytotoxic drug. This can be achieved through a combination of controlling particle size (< 100 nm), high drug loading, low bilayer permeability (by including high transition temperature lipids and cholesterol) and a near neutral surface charge and/or PEGylation (Allen and Cullis, 2013). In addition to the delivery of traditional small molecules, lipid-based nanoparticles can be used to deliver nucleic-based drugs; patisiran (Onpattro®; Alnylam), approved by the Food and Drug Administration (FDA) and the European Medicines Agency (EMA) in 2018, is the first small interfering RNA-based drug approved. Patisiran is indicated for the treatment of polyneuropathy of hereditary transthyretin-mediated amyloidosis. As a finished product, it is a solution for infusion containing 2.0 mg/mL of patisiran (a double stranded small interfering ribonucleic acid (siRNA) which is the active substance) incorporated into lipid nanoparticles in a phosphate buffer. The nanoparticles are 60 – 100 nm in size and designed for delivery to hepatocytes. The nanoparticles are formed from a mixture of siRNA and four lipid excipients: 1,2-distearoyl-sn-glycero-3-phosphocholine (DSPC), cholesterol, (6Z,9Z,28Z,31Z)-heptatriaconta-6,9,28,31-tetren-19-yl-4-(dimethylamino)butanoate (DLin-MC3-DMA) and (R)-2,3-bis(tetradecyloxy)propyl 1-(methoxypoly(ethylene glycol)20000)propyl carbamate (DMG-PEG2000). Both DSPC and cholesterol are well known pharmaceutical ingredients whilst DLin-MC3-DMA and DMG-PEG2000 are novel excipients. Each 1 mL of patisirin contains 3.3 mg DSPC, 6.2 mg cholesterol, 13.0 mg DLin-MC3-DMA and 1.6 mg of DMG-PEG2000 and these lipids associate with the siRNA to form lipid nanoparticles which protects the siRNA from immediate degradation in the circulation and improves delivery to the target site in the liver (EMA, 2018).

Staggered Herringbone Micromixer (SHM)	Toroidal Mixer (TrM)
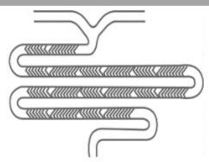	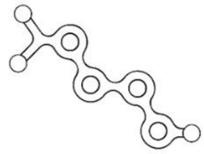
Flow rate capacity 1 – 20 mL/min	Flow rate capacity 1 mL to > 20 L/h
Platform used: • NanoAssemblr Benchtop®	Platform used: • Ignite™ • NxGen Blaze™ • GMP system
Parallelisation of multiple SHM required to achieve GMP scalability	One chip required to achieve GMP scalability
> 100 cited publication using the SHM micromixer	

Figure 1: Micromixer cartridge designs used within these studies. Schematics illustrate the staggered herringbone micromixer (SHM) with embossed chevrons allowing consistent fluid mixing and the toroidal mixer (TrM) with planar geometry employing centrifugal forces to encourage uniform mixing allowing for greater fluid stream velocities. The flow rate capacities for each of the microfluidic mixers and the microfluidic platforms that are used are listed.

1.1 Manufacturing of liposomes and lipid-based nanomedicines

Liposomes and lipid-based nanomedicines are generally produced through a series of size reduction methods (e.g. homogenisation or extrusion) being applied to large liposomes which are initially formed through a lipid hydration process. For example, both AmBisome® and Caelyx® can be produced via an initial lipid hydration step to form liposomes and then the liposomes are reduced to the required size via high pressure homogenisation. In the case of AmBisome®, the active pharmaceutical ingredient (API; amphotericin B), is

Table 1: Process considerations and critical process parameters to consider in microfluidic production of liposomes and LNPs

Process Parameters	Factors to consider	References
Solvent selection	Suitability of solvent for large-scale production. Lipid(s) solubility in the given solvent. Polarity of the solvent can impact of particle size.	(Joshi et al., 2016); (Webb et al., 2019); (van Ballegooie et al., 2019)
Aqueous buffer	Aqueous buffer strength can be used to control particle size.	(Lou et al., 2019)
Lipid concentration	Initial lipid concentration can impact on particle size.	(Dimov et al., 2017); (Forbes et al., 2019)
Production flow rates	Flow rate can impact on particle size	(Guimaraes Sa Correia et al., 2017); (Jahn et al., 2007)
Aqueous to alcohol mixing ratio	Mixing ratio can impact on: • particle size, • drug loading, • drug release.	(Forbes et al., 2019); (van Ballegooie et al., 2019); (Zhigaltsev et al., 2012); (Lin and Malmstadt, 2019)
Operating temperature	Microfluidic production of liposomes does not need to be conducted above the transition temperature of lipids.	(Forbes et al., 2019)

very poorly soluble in aqueous media and is thus formulated by entrapping the drug within the phospholipid membrane of the liposomes (Rivnay et al., 2019). However, amphotericin B also has low solubility in solvents commonly used in the production of liposomes. Thus, a drug-lipid complex is initially formed between amphotericin B and distearoyl-phosphatidylglcercol (DSPG) after acidification of DSPG and then subsequently the remaining lipid components (hydrogenated phosphatidylcholine and cholesterol) are mixed in (Olson et al., 2008). This lipid mixture is then spray-dried to remove the solvent. This spray dried powder is subsequently hydrated in aqueous media and the large vesicles formed are reduced to small unilamellar vesicles through a high shear processor. Throughout this process, the drug remains within the liposomal bilayers. In contrast, with Caelyx®/Doxil®, the API (doxorubicin) is loaded into the liposomes using a transmembrane pH gradient after the liposomes are produced. In this approach, liposomes are produced in suspension with e.g. ammonium sulfate or citrate within the aqueous core of the liposomes. Once the liposomes are down-sized, the liposome suspension is subjected to buffer exchange thus creating the transmembrane pH gradient (high pH outside the liposomes, low pH inside the liposomes). To load the drug, the liposomes are then mixed with doxorubicin; the pH gradient drives amphipathic weak bases such as doxorubicin into the preformed liposomes to promote high (>90%) drug loading (Barenholz, 2012; James et al., 1994; Zhang et al., 2020).

As can be seen, with these products, the production process can be described as 'top-down' with the initial production of large multilamellar vesicles which are then subsequently down-sized. This generally limits production to multiple batch-scale production with low to medium throughput and high cost. Furthermore, passive incorporation of drugs within the aqueous core (without the aid of a transmembrane gradient) is low with these production methods (<10%) and the down-sizing steps can result in degradation of biologicals including proteins, peptides and nucleic acids. In contrast, for the production Onpattro®, the manufacturing process uses microfluidics to promote rapid mixing of lipids in ethanol with siRNA in aqueous media at low pH (pH 4). This mixing process results in a rapid dilution of the ethanol and the formation of the nanoparticles without the need of additional size-reduction steps (Akinc et al., 2019) and overall the manufacturing process is described in five main steps: 1) preparation of active substance (in aqueous buffer) and lipid solutions (in ethanol), 2) mixing of the two solutions to form lipid nanoparticles (LNPs), 3) ultrafiltration, exchange of buffer and initial concentration, 4) dilution to final concentration and bioburden filtration and 5) sterile filtration and filling (EMA, 2018). It has been proposed that these nanoparticles may be better defined as lipid nanoparticles, as opposed to liposomes, given they may not comprise of a lipid-bilayer structure and cryo-TEM tends to show images of spherical nanoparticles with a high electron density core. However, although Onpattro® is described as an LNP and not a liposome formulation, the physico-chemical attributes described in the draft 'FDA Guidance for Industry: Liposome Drug Products (October 2015)' was referenced when characterising the physico-chemical attributes of the LNP in the Onpattro® finished product (EMA, 2018).

1.2.1 Microfluidics as a production method for nanomedicines

Microfluidic manufacturing offers new opportunities for the production of liposomes and lipid-based nanomedicines by providing rapid and controlled mixing of solutions and controlled nanoprecipitation as demonstrated with the production of LNPs such as Onpattro®. The first use of microfluidic mixing to produce liposomes was described by Jahn et al., where the authors reported the use of hydrodynamic focusing of lipids dissolved in water miscible alcohol between two aqueous buffer streams in a microfluidic cartridge. This produced monodispersed liposomes, with their particle size being controlled by the flow rate (Jahn et al., 2004). A refinement of this process was subsequently developed by Zhigaltsev et al. based on a staggered herringbone mixer (SHM; Figure 1) (Belliveau et al., 2012; Evers et al., 2018; Zhigaltsev et al., 2012). Using microfluidic mixers, lipids in a solvent are mixed with an aqueous buffer system. As a result, the polarity is increased and liposomes are formed through the nanoprecipitation of individual monomers into small unilamellar vesicles. The rate of change in polarity during this process can impact on the liposome attributes and as such is influenced by the solvent choice (Webb et al., 2019), buffer concentration (Lou et al., 2019) and the ratio of aqueous phase relative to the alcohol phase (Forbes et al., 2019; Joshi et al., 2016; Roces et al., 2019b). For instance, by using lower polarity solvents such as isopropanol compared to methanol, the rate of polarity change during mixing is reduced and this results in larger vesicle formation (Webb et al., 2019). Similarly, by increasing the flow rate ratio of aqueous buffer to alcohol, liposome size is often reduced (Forbes et al., 2019; Joshi et al., 2016; Roces et al., 2019b). Table 1 summaries the critical processing parameters that should be considered when designing a microfluidic production process.

1.2.2 Micromixer design

When considering fluid mixing, fluid flow can occur in one or two ways: laminar flow or turbulent flow. Either can occur depending on the velocity and viscosity of the fluid. Mixing in macroscopic flow is generally turbulent (Rudyak and Minakov, 2014). However, microflows are more commonly laminar, and mixing under standard conditions involves molecular diffusion processes only, which is generally extremely inefficient

(Kamholz and Yager, 2001; Lee et al., 2016; Rudyak and Minakov, 2014). Therefore, to address this, micromixers have been optimised in terms of channel geometry and architecture. External fields (e.g. acoustic) have also been considered as mechanisms to disrupt fluid streams (Le The et al., 2015). A range of micromixer designs and the nanomedicines produced have been outlined in Table 2. For example, chaotic advection can be created with the use of a staggered herringbone micromixer (SHM; Figure 1). With this design, the fluid streams are passed over a series of protruding herringbone structures causing chaotic flow that creates transverse vortices that are repeatedly changed because of the asymmetric geometry (Tóth et al., 2014). This leads to faster and more refined mixing performances and more homogenous particle sizes when used to produce liposomes (Belliveau et al., 2012; Jahn et al., 2007). This design has been used to produce size-controlled liposomes (Zhigaltsev et al., 2012) with the liposome size being controlled by alterations in flow rate and flow rate ratios (Belliveau et al., 2012; Zhigaltsev et al., 2012), and this has resulted in numerous examples of effective nanomedicine production using this micromixer design (Figure 1). However, this design has some limitations; the need for fabricating consistent herringbone structures at the micro-scale leads to complicated and expensive processes. In addition to this, due to the multi-dimensional dependencies and practical limitation on the size of the herringbone features, it is difficult to achieve the throughput speeds that meet Good Manufacturing Practice (GMP) standards in terms of the final product volume. To address this, an alternative design based on a toroidal mixer design (TrM; Figure 1) has been developed by Precision NanoSystems Inc. This design offers comparable mixing efficiencies under laminar flow at high fluid speeds by using circular structures within the flow path. This induces chaotic advection through increasing the number of vortices and centrifugal forces created between the columns within the cartridge, allowing for improved mixing and also allowing for higher throughput (Lee et al., 2016). Therefore the aim of our work was to compare and map the critical process attributes of both the staggered herringbone mixer that we have previously used (e.g. Anderluzzi and Perrie, 2019; Khadke et al., 2019; Lou et al., 2019; Roces et al., 2019a) with this new toroidal micromixer design and to test the production of liposomes from bench to GMP-scale.

Table 2: Examples of nanoparticles produced using microfluidics.

Microfluidic architecture	Formulation	Entrapped material	Z-average diameter (nm)	Reference
Staggered herringbone mixer	POPC	Doxorubicin	20 – 30	(Zhigaltsev et al., 2012)
	DLinkE2-DMA:DSPC:Chol:PEG-c-DMA	Si-RNA	30 - 55	(Belliveau et al., 2012)
	DSPC:Chol	Metformin and Glipizide	50 - 60	(Joshi et al., 2016)
	DMPC:Chol / DSPC:Chol	Atenolol and quinine	200 – 360	(Guimaraes Sa Correia et al., 2017)
	Span80:Chol / Tween85:Chol	Curcumin	70 – 230	(Obeid et al., 2019)
	Span60:Chol:Cremophor®(EL P or RH40) / Span60:Chol:Solutol®HS15	Cinnarazine	1200 - 5300	(Yeo et al., 2018)
	PLGA / PEG - PLGA	Curcumin	120 - 240	(Morikawa et al., 2018)
	ATX:DSPC:Chol:DMG-PEG:PEG2000	Si-RNA	40 – 50	(Yanagi et al., 2016)
T-mixer	Triolein:POPC:PEG-DSPE	Iron oxide	35 - 140	(Kulkarni et al., 2017)
	PMMA:Cremophor:ELP	Ketoprofen	220 - 360	(Ding et al., 2019)
	PMMA:Eudragit S100:Pluronic F68	Paclitxel	105 - 140	(Dobhal et al., 2017)
	Chitosan Poloxamer 407:HMPC:SDS:Tween20	CRS 74	590 – 920	(de Paiva Lacerda et al., 2015)
	PVPVA:Poloxamer 407:Poloxamer 188	Itraconazole	100 – 300	(Zhang et al., 2018)
Y - type	Ethyl cellulose:Tween80	Losartan potassium	360	(Patil et al., 2015)
HPIMM	PMMA:Cremophor:ELP	Ketoprofen	140 – 200	(Ding et al., 2019)
K-M	PMMA:Cremophor:ELP	Ketoprofen	120 - 260	(Ding et al., 2019)
Hydrodynamic flow focussing	PLGA	Ribavirin	45 - 70	(Bramosanti et al., 2017)
	PLGA	Dexamethasone	200	(Chronopoulou et al., 2014)
	DMPC:Chol:PEG2000-PE	Doxorubicin	80 - 190	(Hood et al., 2014)

1-palmitoyl-2-oleoyl-sn-glycero-3-phosphocholine (POPC); 1,2-distearoyl-sn-glycero-3-phosphocholine (DSPC); Chol (Cholestrol); 1,2-dimyristoyl-sn-glycero-3-phosphocholine (DMPC); e Cremophor® ELP (purified polyoxyl 35 castor oil); Cremophor® RH40 (hydrogenated polyoxyl 40 castor oil); Solutol® HS15 (polyoxyl 15 hydroxystearate); poly(lactic-co-glycolic acid) (PLGA); Polyethylene glycol (PEG); ATX (proprietary ionizable amino lipids); DMG-PEG2000 (1,2-Dimyristoyl-sn-glycerol, methoxypolyethylene glycol, PEG chain molecular weight: 2000; 1,2-distearoyl-sn-glycero-3-phosphoethanolamine-N-[amino(polyethylene glycol)-2000] (*DSPE*-PEG(2000)); Poly(methyl methacrylate) (PMMA); Pluronics F68 (Poloxamer 188, poly(ethylene oxide)–poly(propyleneoxide); hydroxypropyl methylcellulose (HPMC*)*; Sodium dodecyl sulfate (SDS); Polyvinylpyrrolidone vinyl acetate (PVPVA); PEG2000-PE (1,2-dimyristoyl-sn-glycero-3-phophoethanolamine-N-[methoxy(PEG)-2000].

2. Materials and methods

2.1 Materials

The lipids 1,2-distearoyl-sn-glycero-3-phosphocholine (DSPC), hydrogenated soy phosphatidylcholine (HSPC) and 1,2-distearoyl-sn-glycero-3-phosphoethanolamine-N-[methoxy(polyethylene glycol)-2000] (mPEG:DSPE 2000) were obtained from Lipoid GmbH, Ludwigshafen, Germany. 1,2-dimyristoyl-*sn*-glycero-3-phosphocholine (DMPC), 1,2-dioleoyl-*sn*-glycero-3-phosphoethanolamine (DOPE), 1,2-dioleoyl-sn-glycero-3-phospho-L-serine (sodium salt) (DOPS), 1,2-dioleoyl-3-trimethylammonium-propane (chloride salt) (DOTAP) and 1,2-dimyristoyl-rac-glycero-3-methoxypolyethylene glycol-2000 (DMG-PEG2000) were obtained from Avanti Polar Lipids Inc., Alabaster, AL, US. DLin-MC3-DMA was purchased from Biorbyt (Biorbyt Limited, Cambridge, UK). PLGA 50:50 (30,000-60,000 Mw ester terminated), cholesterol (Chol), tristearin, ovalbumin (OVA), phosphate buffered saline (PBS; pH 7.4) in tablet form, doxorubicin (DOX) hydrochloride, ammonium sulfate (AS) polyadenylic acid (PolyA) and the phospholipid assay kit were purchased from Sigma Aldrich Company Ltd., Poole, UK. 1,1'-dioctadecyl-3,3,3',3'-tetramethylindocarbocyanine perchlorate (DilC) was obtained from Fisher Scientific, Loughborough, England, UK. Tris (hydroxymethyl) aminomethane (TRIS) was obtained from ICN Biomedicals, Inc. For OVA purification by tangential flow filtration (TFF), modified polyethersulfene (mPES) hollow fibre columns were used (100 - 750 kD MWCO depending on formulation; Spectrum Inc., Breda, The Netherlands). For the release studies, Biotech CE Tubing MWCO 300 kD was used (Spectrum Inc., Breda, The Netherlands). HPLC grade methanol, 2-propanol, acetonitrile and Pierce™ Micro BCA Protein Assay kit were purchased from Fisher Scientific, Loughborough, England, UK. All solvents were HPLC grade.

2.2 Microfluidic manufacture of liposomes

Microfluidic production of liposomes was achieved using either the NanoAssemblr® Benchtop, the Ignite™ or NxGen Blaze™ platforms (Precision NanoSystems Inc, Vancouver, Canada). In these systems different microfluidic mixers were used: a staggered herringbone (SHM) or a toroidal mixer (TrM) (NanoAssemblr

Classic or NxGen™ respectively) as outlined in Figure 1. Initial lipid concentrations used were 4 to 40 mg/mL depending on the formulation. Lipids were dissolved in either methanol or ethanol and PGLA 50:50 was dissolved in acetonitrile and mixed with an aqueous phase. For the production of protein loaded liposomes, varying initial concentrations (0.25 – 1 mg/mL in PBS; 10 mM, pH 7.4) of OVA were used as the aqueous phase. For pH gradient loaded liposomes, ammonium sulfate (250 mM) was used as the aqueous phase. For PolyA loaded liposomes, PolyA dissolved in TRIS (10 mM; pH 7.4) at an initial concentration of 166 µg/mL. Microfluidic mixing was undertaken at a range of flow rate ratios (FRR) from 1:1 to 5:1 (aqueous:alcohol phase) and at total flow rates (TFR; the production speed) from 10 to 60 mL/min depending on the system.

2.2.1 GMP microfluidic production of liposomes.

GMP microfluidic production of liposomes was achieved using the NanoAssemblr GMP system and a TrM (NxGen 500) cartridge which uses the same toroidal mixer design with inline dilution and with custom HPLC pumps. Liposomes were manufactured at a FRR of 3:1 and a TFR of 200 mL/min.

2.3 Down-stream production and purification of nanoparticle and liposomal formulations using tangential flow filtration

Solvent and unentrapped drug (protein and doxorubicin depending on the formulation) were removed from liposome suspensions using the Krosflo Research IIi tangential flow filtration (TFF) system with a 100, 500 or 750 kD mPES column and a 12 diafiltrate volume. The system was run at 21 mL/min. With GMP production, a 100 kD mPES filter was used. For liposomes entrapping protein, liposomes were washed in PBS. For liposomes actively loaded with doxorubicin, liposomes were prepared encapsulating ammonium sulfate 250 mM using microfluidics. Purification and establishment of a pH gradient between the interior and the exterior of the liposomes was carried out using TFF and washing with PBS (pH 7.4). Doxorubicin was subsequently loaded into the liposomes (10 min, 60°C) and non-encapsulated doxorubicin was removed using TFF again and washing with PBS. For liposomes with entrapped PolyA, ethanol concentrations were reduced to 5% by diluting samples 1 in 10. The applicability of TFF for down-stream processing of other nanoparticles was also tested; physico-chemical characteristics were compared before and after TFF to access the impact of downstream processes on various formulations. Liposomal formulations including DSPC:Chol (2:1 w/w), DSPC:Chol:DOPS (10:5:4 w/w) and DSPC:Chol: DLin-MC3-DMA:DMG-PEG2000 (14:32:45:9 w/w) were prepared using an initial lipid concentration of 4 mg/mL. DSPC:Chol and DSPC:Chol:DOPS were prepared at a FRR of 3:1 and TFR of 15 mL/min and initial OVA concentration of 0.25 mg/mL. The ionisable lipid formulation (containing DLin-MC3-DMA) and DOPE:DOTAP were prepared at 1:1 FRR and TFR of 10 mL/min. For HSPC:Chol:DSPE-PEG2000 (3:1:1 w/w) liposomes an initial concentration of 10 mg/mL was used with a FRR of 1.5:1 at 12 mL/min and doxorubicin was subsequently loaded at 0.125 g/g lipid of preformed liposomes. For the nanoparticle formulations, OVA loaded tristearin and mPEG-DSPE2000 (5:1 w/w) were manufactured at a TFR of 15 mL/min and FRR 3:1 with an initial OVA concentration of 0.25 mg/mL. PLGA 50:50 (10 mg/mL initial) was produced at 1:1 FRR and TFR 10 mL/min with Tris buffer as the aqueous phase. All formulations were characterised before and after TFF purification by dynamic light scattering (DLS) in terms of hydrodynamic size (Z-average), PDI and zeta potential. Post purification, loading within the systems and product recovery was measured. Liposome recovery was quantified by incorporating DilC at 0.2 mol% into the bilayer of the liposomes with the sample fluorescence measured before and after TFF allowing the lipid quantification to be calculated by referring to a calibration curve. PLGA product yield was measured using a bicinchonic acid (BCA; Thermo Fisher Scientific, Waltham, MA, USA) assay kit. Due to the incompatibility of the column with acetonitrile, dialysis was performed prior TFF. To calculate the nanoparticle yield, a calibration curve using the dialysed sample was used and nanoparticle yield was measured as percentage recovered compared to the dialysed nanoparticles. 25 µL sample and 200 µL of BCA working reagent were added into the wells, the plate was incubated at 37°C for 30 min and the absorbance was measured at 564 nm (as per manufacturer's instructions).

2.4 Product characterisation

2.4.1 Particle size attributes

Particle size (Z-average diameter), polydispersity index (PDI) and zeta potential were measured by dynamic light scattering using a Zetasizer Nano ZS (Malvern Panalytical Ltd, Worcestershire, UK) equipped with a 633 nm laser and a detection angle of 173°. The samples were measured and the values of water were used for refractive index and viscosity. Zetasizer Software v.7.11 (Malvern Panalytical Ltd.) was used for the acquisition of data. All measurements were undertaken in triplicate with the attenuation value between 6 and 9.

2.4.2 Lipid concentration quantification

Lipid recovery was accessed using DilC (excitation and emission, 549 and 565 nm respectively) or for DSPC:Chol protein-loaded liposomes a commercial colorimetric phospholipid assay (Sigma Aldrich Company Ltd., Poole, UK) was used. For phospholipid concentrations determined using the commercial colorimetric phospholipid assay (Sigma Aldrich Company Ltd., Poole, UK) the manufacturer's recommendations were followed. Briefly, a calibration curve was produced by diluting the included standard to 0.5 mM and adding varying standard volumes to a 96 well plate in duplicate and completing the final volume per well to 50 µL with deionised water. 50 µL of solubilised phospholipids were diluted 1:50 with purified water while liposome samples before and after tangential flow filtration were diluted 1:10 with purified water. 50 µL of reaction mix containing the assay buffer, enzyme mix, phospholipase D enzyme and dye reagent, as per manufacturers recommendations, was added to each sample which were then incubated at room temperature for 30 min. Absorbance was measured at 562 nm using a Bio-rad 680 microplate reader. For the other formulations mentioned, lipid recovery was performed by incorporating DilC at 0.2 mol% into the bilayer of the liposomes with the sample fluorescence measured before and after TFF allowing the lipid quantification to be calculated.

2.4.3. Protein entrapment efficiency.

Solubilisation of liposomes to release entrapped protein and subsequent protein quantification was achieved following a modified published protocol (Forbes et al., 2019). Briefly, a solubilisation mixture (PBS:2-Propanol 1:1 v/v) was added to liposome samples at a 1:1 v/v ratio and vortexed. Protein loading was quantified using either the micro-BCA (Thermo Fisher Scientific, Waltham, MA, USA) or reversed-phase high performance liquid chromatography (RP-HPLC, Shimadzu 2010-HT, Milton Keynes, UK) with a Jupiter 5 µm C5 300A column 4.6 mm i.d. x 250 mm length (Phenomenex, UK). A flow rate of 1 mL/min was used with an injection volume of 100 µL and run temperature of 35 °C. A gradient flow mobile phase was used (0.1%TFA in water (A), 0.1%TFA in acetonitrile (B); A/B from 95:5 to 35:65 in 20 min) gradient flow mobile phase was used (0.1%TFA in water (A), 0.1%TFA in acetonitrile (B) (Umrethia et al., 2010)) and an OVA retention time of 10 – 14 min using a UV detector at 210 or 280 nm. A linear calibration curve was obtained using a range of OVA concentrations (0 – 1 mg/mL) and liposomes (4 mg/mL). All calibration curves produced by RP-HPLC and micro-BCA for protein quantification had a linear regression of > 0.99 and a LOQ < 50 µg/mL.

2.4.4. Doxorubicin encapsulation efficiency

For active loading, doxorubicin was added at 0.125 g/g lipid of preformed liposomes. Doxorubicin stock was prepared at 20 – 30 mg/mL in ultrapure water. Quantification of doxorubicin was performed using a microplate reader model 680 (Bio-rad Laboratories. Inc., Hertfordshire, UK) measuring the UV absorbance at 490 nm. Liposomes were solubilised with 50% 2-propanolol (1:1 v/v). Calibration curves were performed under the same conditions as the sample. A linear calibration curve was obtained (R^2=0.997) from 0 – 0.5 mg/mL doxorubicin with an LOD and LOQ of 0.03 and 0.1 mg/mL respectively.

2.4.5 PolyA entrapment efficiency

PolyA encapsulation efficiency (EE%) was measured using Quant-iT™ RiboGreen™ RNA Assay Kit (Invitrogen™). Briefly, 100 µL of the diluted fluorescent dye was added to 100 µL liposomes and incubated in absence of light for 5 min. Non-encapsulated PolyA was quantified by measuring fluorescence (λem= 480 nm, λex= 520nm) using a fluorimeter (Polarstar Omega, BMG Labtech). A linear calibration curve was obtained (R^2=0.997) from 0 – 1000 ng/mL PolyA with LOD and LOQ of 75 and 228 ng/mL respectively.

2.4.6 Cryo-TEM imaging of liposomes

Samples were prepared using a Gatan CP3 Cryoplunge by depositing liposomes (3 µL) onto a 300 mesh copper TEM grid (graphene oxide / holey carbon or holey carbon) held in tweezers in a controlled environment (~ 23 °C, 80% humidity), blotted for 1.5 s then plunged into liquid nitrogen cooled liquid ethane (-172 °C) to vitrify. Samples were maintained under liquid nitrogen until transfer to the TEM (Gatan 926 cryo sample holder) and held at -176 °C during analysis (Gatan Smartset model 900 controller). Images of liposomes were recorded using a JEOL 2100 Plus operating at 200 kV (Gatan Ultrascan 100XP camera).

2.5 Protein release from liposomes

DSPC:Chol liposomes (2:1 w/w) entrapping OVA were produced at a flow rate ratio of 3:1, a flow rate of 15 mL/min, an initial lipid concentration of 16 mg/mL (dissolved in methanol) and 1 mg/mL initial OVA (in PBS). Initial protein loading for all liposome samples were in the range of 215 to 220 µg/mL with no significant difference between the SHM and TrM samples and thus 1 mL of each purified formulation was placed in a 300 kD dialysis bag in the presence of 20 mL PBS (pH 7.4 ± 0.2), n = 3 for each micromixer. The samples were incubated at 37 °C with agitation and at 0, 24, 48, 72 and 120 h, 100 µL of the liposome sample was removed and replaced with an equal volume of buffer. The protein content within the liposomes was quantified using the described RP-HPLC method. Release studies were conducted up to 80% release was achieved; above this level, protein concentration within the liposomes fell below the LOQ (50 µg/mL) and could not be quantified.

2.6 Statistical analysis

Results are represented as mean ± SD with n = 3 independent batches. ANOVA tests were used to assess statistical significance, with a Tukey's post adhoc test (p value of less than 0.05). Where appropriate, the similarity or differences between drug release profiles between formulations was assessed by the f_2 similarity test.

3. Results

3.1 Bench-scale production of liposome formulations using different microfluidic mixers

Given that the new toroidal mixer supports the transition from bench-scale at low volumes (1 mL) through to GMP production (>20 L/h) (Figure 1), initial studies focused on mapping across from the staggered herringbone design mixer to the toroidal mixer. Figure 2 outlines initial studies comparing the size, PDI and zeta potential attributes of anionic, neutral and cationic liposomes prepared using both types of microfluidic mixers. Figure 2 demonstrates that across all three liposome formulations tested, the key physico-chemical attributes map across between the two types of microfluidic mixers with no significant difference in size, PDI (Figure 2A) and zeta potential (Figure 2B). Anionic liposomes (DSPC:Chol:DOPS; 10:5:4 w/w) were 55 – 60 nm with a zeta potential of -20 to -25 mV irrespective of the microfluidic mixer used (Figure 2). Neutral liposomes (DSPC:Chol; 2:1 w/w) were slightly smaller in size (~40 nm) and near neutral in terms of zeta potential and again the choice of micromixer used had no impact on these attributes. Similarly, with the cationic liposomes (DOPE:DOTAP; 1:1 w/w), there was no significant difference in size (50 – 60 nm) or zeta potential (~45 mV) (Figure 2) for liposomes produced using the staggered herringbone or the toroidal micromixer.

When these liposomes formulations were loaded with either OVA protein (anionic and neutral liposomes) or polyA (cationic liposomes) the particle size, PDI, loading and zeta potential again showed no significant differences between liposomes prepared by the staggered herringbone or the toroidal microfluidic mixer

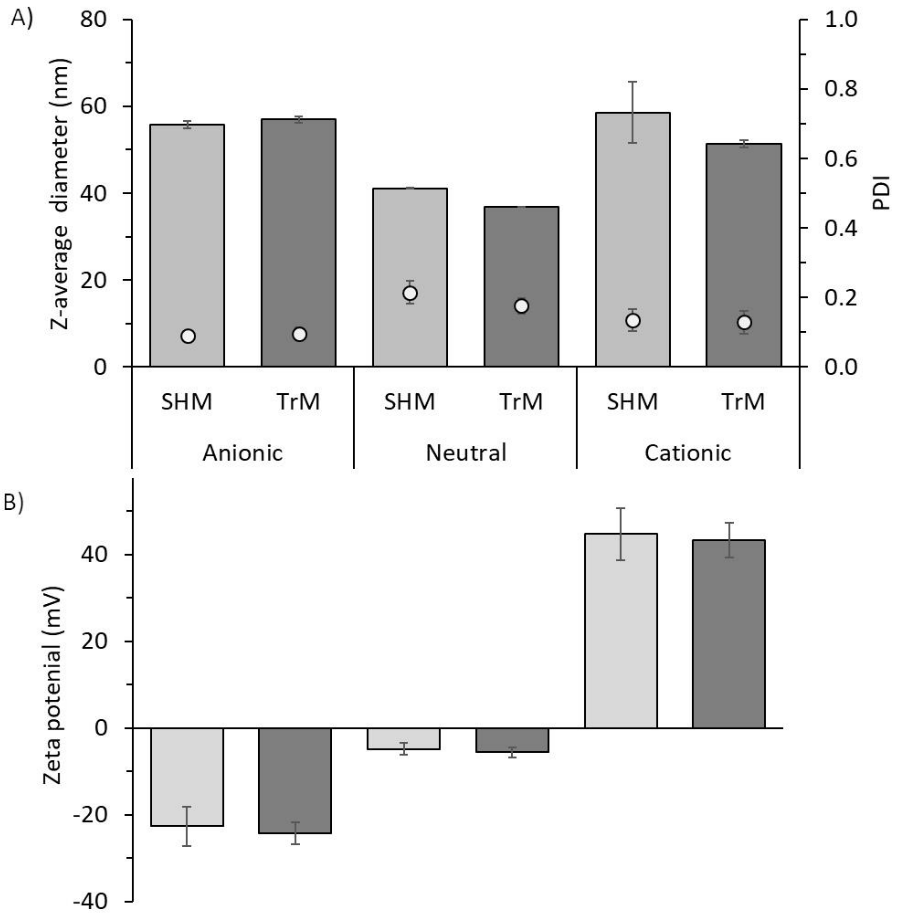

Figure 2: Comparison of micromixer design on the physio-chemical attributes of liposomes. Liposomes were prepared using either a staggered herringbone (SHM) in the NanoAssemblr® Benchtop or a toroidal mixer (TrM) in the Ignite™ and their physico-chemical attributes compared. Anionic liposomes (DSPC:Chol:DOPS 10:5:4 w/w) and neutral liposomes (DSPC:Chol 2:1 w/w) were prepared at a 3:1 flow rate ratio and a total flow rate of 15 mL/min and purified by tangential flow filtration. Cationic liposomes DOPE:DOTAP (1:1 w/w) were produced at a flow rate ratio of 1:1 and a total flow rate of 10 mL/min and purified using a 1/10 dilution with Tris to reduce the solvent concentrations. All formulations were prepared at an initial lipid concentration of 4 mg/mL dissolved in ethanol (DOPE:DOTAP) and methanol (DSPC:Chol:DOPS and DSPC:Chol). The liposome z-average diameter (columns) and PDI (open circles) (A) and zeta potential (B) were measured. Results represent mean ± SD of three independent batches.

(Figure 3). OVA was loaded into neutral and anionic liposomal formulations that we have investigated previously as potential protein and vaccine delivery systems (Forbes et al., 2019; Webb et al., 2019). With cationic systems, the majority of the work is focused on nucleic acid delivery, hence PolyA was used as a surrogate for RNA. With the anionic liposomes, protein loading was approximately 20% of initial amount added, whilst neutral liposomes had a higher protein loading (approximately 35%) irrespective of the micromixer used. When loaded with protein, anionic liposomes tend to increase in size and have reduced protein loading compared to neutral liposomes, presumably due to the electrostatic repulsion between the anionic protein and the anionic bilayer membranes (Forbes et al., 2019; Webb et al., 2019). With the cationic formulations, due to electrostatic interactions between the cationic lipid and polyA, loading was high (95-100%), again irrespective of the micromixer used (Figure 3). In terms of particle size, again there was no differences in size; particles produced using the SHM were 58 ± 7 nm and 55 ± 1 nm whereas for TrM were 51 ± 1 and 52 ± 3 for DOPE:DOTAP (Figure 2) and PolyA loaded DOPE:DOTAP particles (Figure 3) respectively.

Unlike conventional liposome production methods, using microfluidics we have previously shown (Forbes et al., 2019; Webb et al., 2019) that liposomes containing lipids with high (e.g. DSPC) or low (e.g. DMPC) lipid phase transition temperatures can be manufactured at ambient temperature without the need to work above lipid transition temperatures. To confirm the new microfluidic mixer design also offers this advantage, three different liposome formulations were prepared containing DMPC, DSPC or HSPC and cholesterol, all at a 2:1 w/w ratio (Figure 4) and loaded with OVA protein. Liposomes containing DMPC:Chol were 80 – 90 nm, DSPC:Chol liposomes were 50 – 60 nm and HSPC:Chol liposomes were 50 – 60 nm, all with PDI of 0.2 or below, with no significant difference between liposomes produced using a staggered herringbone mixer and a toroidal mixer (Figure 4A). Similarly, across all three liposome formulations there was no significant difference in protein loading (30 – 37%) nor zeta potential (-5 to – 10 mV) (Figure 4).

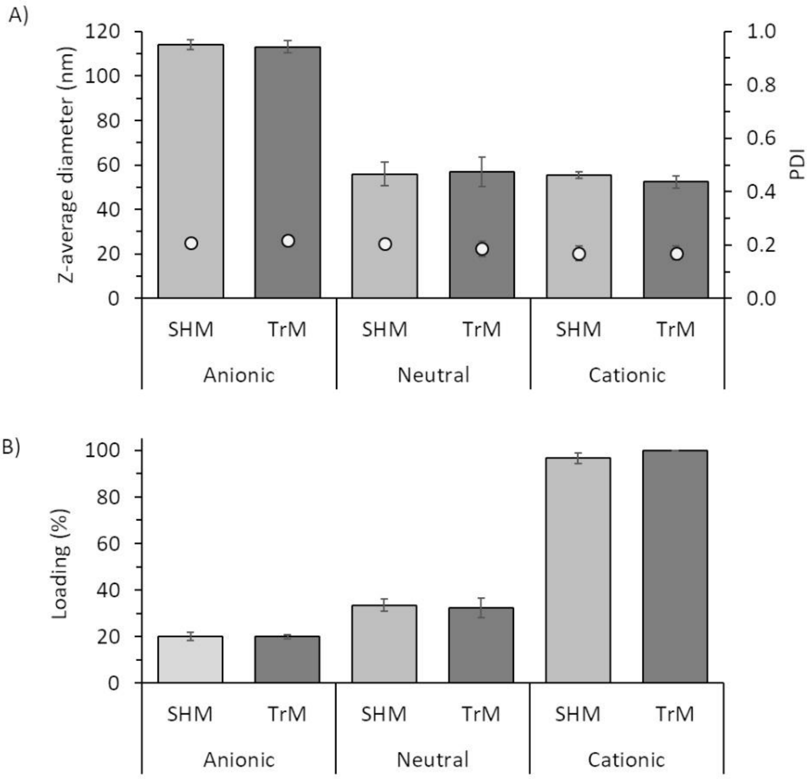

C)

Zeta Potential (mV)	-37 ± 2	- 40 ± 3	-8 ± 2	-7 ± 1	47 ± 4	45 ± 3

Figure 3: Production of drug loaded liposomes using different microfluidic mixers. Liposomes were prepared using either a staggered herringbone (SHM) in the NanoAssemblr® Benchtop or a toroidal mixer (TrM) in the Ignite™. Anionic liposomes (DSPC:Chol:DOPS 10:5:4 w/w) and neutral liposomes (DSPC:Chol 2:1 w/w) were prepared at a 3:1 flow rate ratio and a total flow rate of 15 mL/min. All formulations were prepared at an initial lipid concentration of 4 mg/mL dissolved in methanol and loaded with 0.25 mg/mL initial OVA concentration dissolved in PBS pH 7.4. Non-entrapped protein was removed by tangential flow filtration and protein loading was quantified via RP-HPLC. Cationic liposomes (DOPE-DOTAP (1:1 w/w) were prepared at a flow rate ratio of 1:1 and a total flow rate of 10 mL/min. An initial lipid concentration of 4 mg/mL (dissolved in ethanol) and an initial PolyA concentration of 166 µg/mL (dissolved in Tris buffer pH 7.4, 10 mM) was used. Cationic liposomes were purified by dilution and drug loading quantified by using a Ribogreen assay. The liposome z-average diameter (columns) and PDI (open circles) (A), drug loading (B) and zeta potential (C) were measured. Results represent mean ± SD of three independent batches.

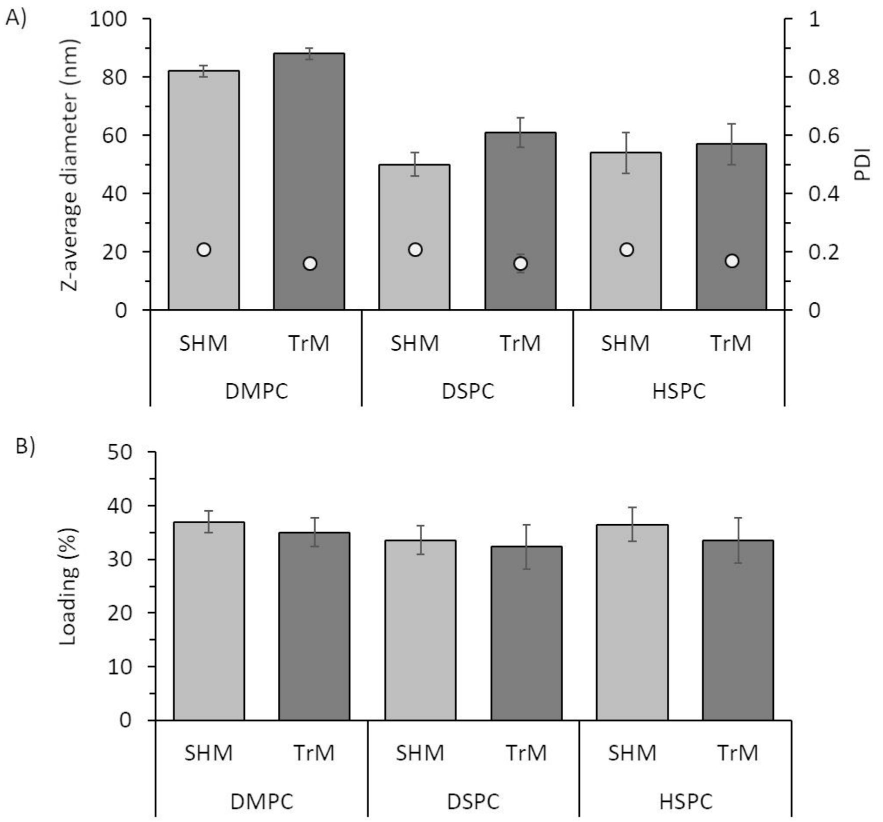

C)						
Zeta potential (mV)	-7 ± 3	-9 ± 1	-5 ± 2	-5 ± 1	-7 ± 2	-9 ± 5

Figure 4: Production of liposomes entrapping protein are room temperature irrespective of phospholipid transition temperature. Liposomes were prepared from DMPC, DSPC or HSPC in combination with cholesterol at a 2:1 w/w ratio using either a staggered herringbone (SHM) in the NanoAssemblr® Benchtop or a toroidal mixer (TrM) in the Ignite™. Liposomes were manufactured at a 3:1 flow rate ratio, 15 mL/min total flow rate, an initial lipid concentration of 4 mg/mL (dissolved in methanol) and an initial ovalbumin protein concentration of 0.25 mg/mL (dissolved in PBS pH 7.4) which was quantified by RP-HPLC after purification. All liposomes were prepared at room temperature. Liposomes were purified by tangential flow filtration. The liposome z-average diameter (columns) and PDI (open circles) (A), loading (B), and zeta potential (C) was compared. Results represent mean ± SD of three independent batches.

3.2 Manufacturing process parameters matched across both microfluidic mixers

Given that the new toroidal mixer was able to produce liposomes with the same physico-chemical attributes (size, PDI, zeta potential and loading) across a range of liposome formulations (Figures 2 to 4), the next step was to confirm that a range of manufacturing process parameters could be mapped across from the staggered herringbone mixer to the new toroidal mixer. To confirm this, the impact of flow rate ratio, total flow rate and solvent selection were tested using liposomes composed of DSPC:Chol (2:1 w/w). From Figure 5, again we see that the liposome attributes in terms of particle size, PDI and protein loading match for liposomes produced using the staggered herringbone and toroidal mixer. Liposomes produced at a 3:1 aqueous:alcohol flow rate ratio were ~ 55 nm, whilst those produced at a 5:1 flow rate ratio tended to be slightly larger (55 – 60 nm) (Figure 5A) with no significant difference between the formulations prepared on the two different mixers. In the same way, loading was not influenced by the choice of mixer, with those produced at 3:1 having a protein loading around 35% whilst those at 5:1 were lower (approximately 30%; Figure 5C). In terms of flow rate, rates of 12 to 20 mL/min were tested using both the staggered herringbone and the toroidal mixer, again there was no significant difference in particle size and PDI (50 – 60 nm, 0.2; Figure 5B) and protein loading (approximately 35%; Figure 5D).

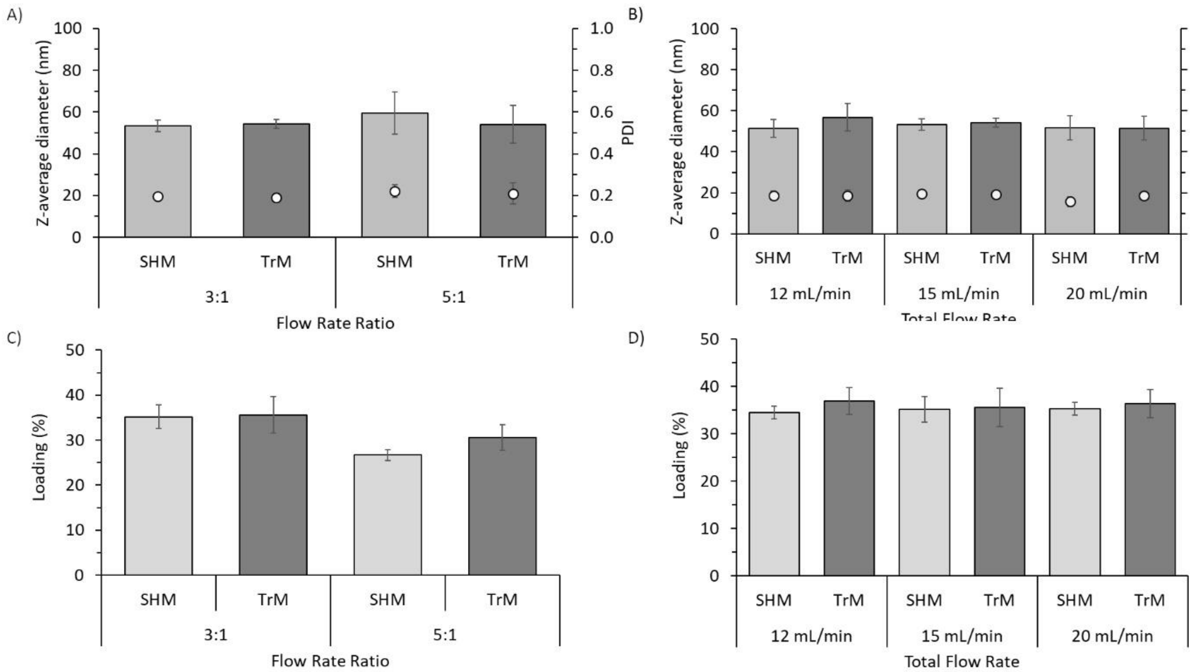

Figure 5: Small-scale production of liposomes using different process parameters. Liposomes (DSPC:Chol 2:1 w/w) were produced by either a staggered herringbone (SHM) in the NanoAssemblr® Benchtop or a toroidal mixer (TrM) in the Ignite™ and the effect of flow rate ratio (A and C) and total flow rate (B and D) investigated on liposome z-average diameter (columns) and PDI (open circles) (A and B) and protein loading (C and D). Liposomes entrapping OVA were manufactured at flow rate ratios of 3:1 or 5:1 and a total flow rates of 12, 15 or 20 mL/min. An initial lipid concentration of 4 mg/mL (dissolved in methanol) and an initial OVA concentration of 0.25 mg/mL (dissolved in PBS) was used. Liposomes were purified by tangential flow filtration and protein loading quantified by RP-HPLC. Results represent mean ± SD of three independent batches.

Equally, when switching between solvents, both microfluidic mixers show similar liposome attributes in terms of size (~55 nm when produced in methanol, and ~60 nm when produced in ethanol), PDI (~0.2), loading (~35%) and zeta potential (-5 to -10 mV) (Figure 6). The impact of lipid concentration was also tested for both micromixers (Figure 6 D and E); the results again show no significant difference between the SHM and TrM in terms of particle size attributes and protein loading. With both microfluidic mixer systems, the particle size remains in the range of 50 to 65 nm with loading 26 – 36 % up to final lipid concentrations of 8 mg/mL (Figure 6D and E). When the final lipid concentration is increased to 10 mg/mL, the particle size increases to approximately 75 nm but the drug loading remains constant (Figure 6D and E respectively) again with no significant difference resulting from the microfluidic cartridge design used.

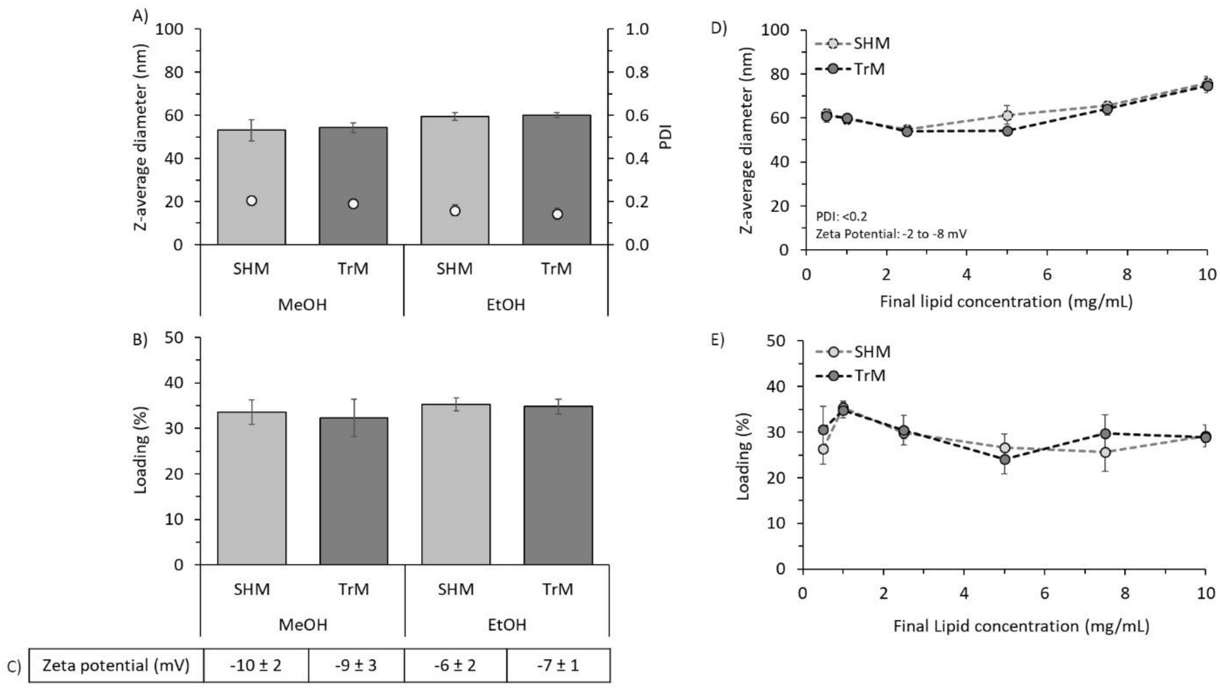

Figure 6: Investigating the impact of solvent choice and lipid concentration when using different microfluidic mixers. Liposomes (DSPC:Chol 2:1 w/w) entrapping OVA were produced using either methanol or ethanol to dissolve the lipid and either a staggered herringbone (SHM) in the NanoAssemblr® Benchtop or a toroidal mixer (TrM) in the Ignite™. The liposome z-average diameter (columns) and PDI (open circles) (A), protein loading (B; quantified by RP-HPLC) and zeta potential (C) was measured. DSPC:Chol liposomes were manufactured using either methanol or ethanol at a flow rate ratio of 3:1, a total flow rate of 15 mL/min, an initial lipid concentration of 4 mg/mL and OVA concentration of 0.25 mg/mL. Liposomes (DSPC:Chol 2:1 w/w) entrapping OVA were also produced at final lipid concentrations from 0.5 to 10 mg/mL and their particle size (D) and protein loading (E) was measured by a combination of RP-HPLC and micro-BCA. Liposomes were purified by tangential flow filtration. Results represent mean ± SD of three independent batches.

In terms of morphological attributes, both microfluidic mixers produced similar small unilamellar vesicles (Figure 7A to D) with the same lipid recovery after microfluidic production (Figure 6E). From the cryo-TEM images, the particle sizes were also calculated with liposomes produced via the staggered herringbone mixer being 51 ± 6 nm (n = 109) whilst those produced via the toroidal mixer being 47 ± 5 nm (n = 227) with no significant difference. These diameters should be slightly smaller than those obtained by DLS; TEM measurements do not include the hydration layer. Protein release profiles from liposomes produced by the two different mixers were also not significantly different (similarity factor (f2) of 65; figure 7F).

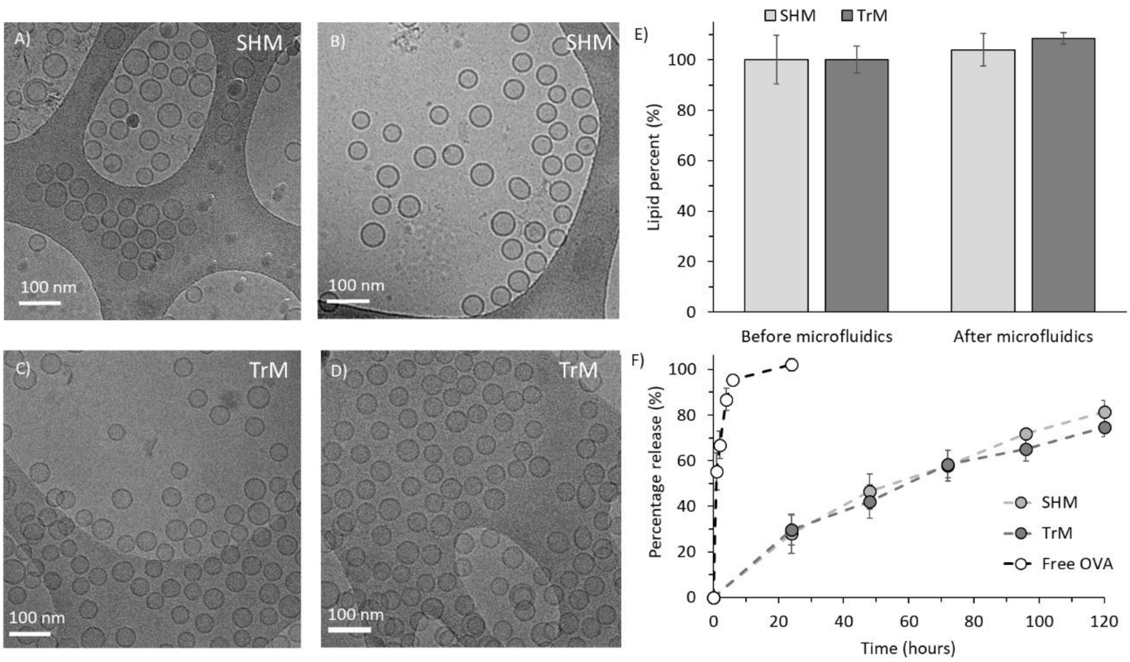

Figure 7: Liposome morphology, lipid recovery and protein release profiles of liposomes produced using different microfluidic mixers. Liposomes (DSPC:Chol 2:1 w/w) entrapping OVA were produced using either a staggered herringbone (SHM) in the NanoAssemblr® Benchtop or a toroidal mixer (TrM) in the Ignite^{TM}. (A) and (B) show the morphology of liposomes produced using the staggered herringbone mixer. (C) and (D) show the morphology of formulations produced using the toroidal mixer. (E) Phospholipid recovery in liposomes produced by each mixer before and after purification via tangential flow filtration. (F) Protein release from liposomes produced by the two different micromixer designs and incubated at 37 °C for 120 h under agitation. DSPC:Chol liposomes were produced at a flow rate ratio of 3:1, and a total flow rate of 15 mL/min. An initial lipid concentration of 4 mg/mL (dissolved in methanol) and an initial OVA concentration of 0.25 mg/mL (dissolved in PBS) was used for (A) to (E). For protein release studies (F), liposome formulations were produced at a 4-folds higher concentration (initial lipid concentration of 16 mg/mL and initial OVA of 1 mg/mL). Protein loading and release was quantified by RP-HPLC. Results represent mean ± SD of three independent batches (E, F).

3.3 GMP production of protein loaded liposomes

Given that at bench-scale the staggered herringbone and toroidal mixer were shown to produce liposomes of the same physico-chemical attributes across a range of formulations (figure 2 to 4) and process parameters (Figures 5 to 7), the next step was to assess the ability to apply the toroidal mixer to produce liposomes at high production rates (>200 mL/min) on a GMP system. To achieve this, we assessed the attributes of DSPC:Chol (2:1 w/w) liposomes entrapping protein (OVA) produced at bench-scale (12 mL/min; Ignite^{TM} platform), to larger preclinical-scale (60 mL/min; NxGen Blaze^{TM} and NxGen 400 Cartridge), through to GMP-scale (NanoAssemblr GMP system and NxGen 500 cartridge) (run at 200 mL/min). The NxGen 500 has a larger cross-sectional area resulting in lower fluidic resistance but necessitating a higher flow rate to achieve the optimal mixing speed. Across all three platforms, the lipids were dissolved in ethanol and purified by tangential flow filtration. Figure 8 shows that the liposomes were 60 – 70 nm with a PDI of ~0.2 across the three flow rates tested (Figure 8A), with similar particle size distribution profiles (Figure 8B) and protein loading (Figure 8C) with no significant difference as we move from small bench-scale (1 mL, 12 mL/min) to GMP-scale (200 mL/min).

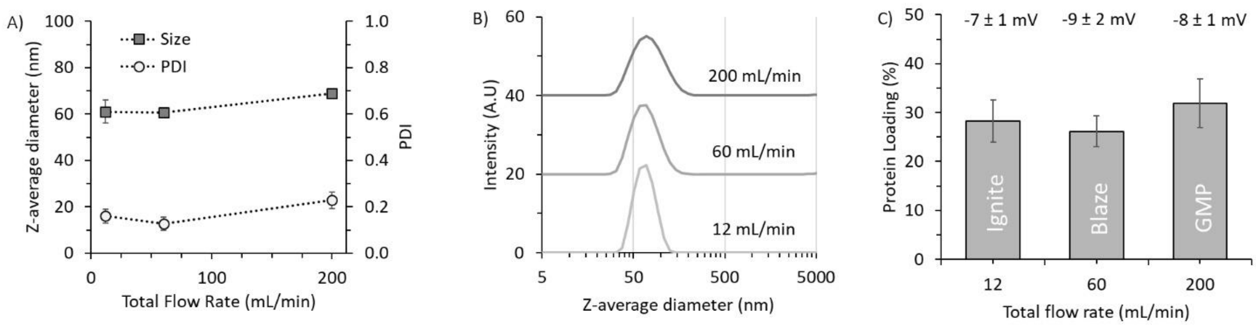

Figure 8: Scale-independent production of liposomes entrapping protein - from bench to GMP. Liposomes (DSPC:Chol 2:1 w/w) entrapping OVA were produced using a toroidal mixer in the Ignite^{TM}, NxGen Blaze^{TM} or a GMP microfluidic manufacturing system. All three systems were run at the same flow rate ratio (3:1). Total flow rate was increased to demonstrate scale-independent production across different systems from 12 mL/min (Ignite^{TM}) to 60 mL/min (NxGen Blaze^{TM}) or 200 mL/min (GMP system). The liposome z-average diameter and PDI (A), intensity-weighted size distribution (B) and protein loading quantified by micro-BCA (C) are shown. Results represent mean ± SD of three independent batches for the Ignite and NxGen Blaze systems and 1 large-scale batch on the GMP system.

3.4 Down-stream processing of nanomedicines

As part of any production process for liposomes and nanoparticles, a purification step is required. For the bench through to GMP production of liposomes, tangential flow filtration was employed to remove solvent and non-entrapped drug (Figures 2 to 8). This process can be applied to a range of liposome and nanoparticle formulations produced by microfluidics as outlined in Table 3. In terms of liposome formulations, neutral liposomes (DSPC:Chol), anionic liposomes (DSPC:Chol:DOPS), PEGgylated liposomes (HPSC:Chol:DSPE-PEG2000) and liposomes formulated using ionisable lipids (DSPC:Chol: DLin-MC3-DMA:DMG-PEG2000) were prepared. Each formulation was characterised before and after purification by tangential flow filtration. Table 3 demonstrates that the particle size, PDI and zeta potential was unchanged by the process and high product recovery (>95% of liposome product) was noted. To test the wider application of this purification process, solid lipid nanoparticles and polymeric nanoparticles were also produced by microfluidics and purified by tangential flow filtration (Table 3). Again, nanoparticle attributes were retained through the purification process with high product yield.

Table 3. Down-stream production and purification of nanoparticle and liposomal formulations using tangential flow filtration.

Liposomes	Pre-TFF purification	Post-TFF purification
DSPC:Chol (2:1 w/w) liposomes incorporating protein (OVA)	Size: 51 ± 3 nm PDI: 0.21 ± 0.07 ZP: -4 ± 1 mV	Size: 58 ± 6 nm PDI: 0.19 ± 0.01 ZP: -6 ± 2 mV Loading: 34 ± 2% Product yield: 103 ± 6%
DSPC:Chol:DOPS (10:5:4 w/w) liposomes incorporating protein (OVA)	Size: 139 ± 26 nm PDI: 0.15 ± 0.03 ZP: -27 ± 4 mV	Size: 127 ± 26 nm PDI: 0.14 ± 0.01 ZP: - 26 ± 3 mV Loading: 16 ± 1% Product yield: 97 ± 3%
HSPC:Chol:DSPE-PEG2000 (3:1:1 w/w) incorporating doxorubicin	Size: 86 ± 7 nm PDI: 0.07 ± 0.02 ZP: -7 ± 2 mV	Size: 85 ± 6 nm PDI: 0.09 ± 0.02 ZP: -10 ± 1 mV Loading: 95 ± 5 % Product Yield: 95 ± 7%
DSPC:Chol: DLin-MC3-DMA:DMG-PEG2000 (14:32:45:9 w/w)	Size: 175 ± 14 nm PDI: 0.07 ± 0.01 ZP: -0.1 ± 0.2 mV	Size: 187 ± 4 nm PDI: 0.08 ± 0.03 ZP: 0.2 ± 0.2 mV Product yield: 100 ± 5%
Nanoparticles		
Solid lipid nanoparticles Tristearin and mPEG-DSPE-2000 incorporating protein (OVA)	Size: 73 ± 4 nm PDI: 0.22 ± 0.01 ZP: -26 ± 5 mV	Size: 76 ± 7 nm PDI: 0.20 ± 0.01 ZP: -16 ± 3 mV Loading: 30 ± 8% Product yield: 96 ± 3%
Polymeric nanoparticles PLGA 50:50	Size: 134 ± 3 nm PDI: 0.07 ± 0.03 ZP: -46 ± 4 mV	Size: 152 ± 5 nm PDI: 0.07 ± 0.03 ZP: -44 ± 6 mV Product yield: 94 ± 10%

Physico-chemical characteristics were compared before and after TFF to access the impact of downstream processes on various formulations. Liposomal formulations, solid lipid nanoparticles and polymeric nanoparticles were all prepared using microfluidic manufacturing (SHM mixer). All formulations were characterised before and after TFF purification by DLS in terms of hydrodynamic size (z-average), PDI and zeta-potential. Post purification, loading within the systems and product recovery was also measured. Results represent mean ± SD of three independent batches.

4. Discussion

For liposomes, and nanomedicines in general to be more widely exploited rapid, cost-effective and scalable manufacturing processes are needed. For the production of nanoparticles, we have two options: 'top-down' (where we make large particles and reduce their size) or 'bottom-up' where the nanoparticles are prepared by controlled nanoprecipitation. In the latter case, microfluidics can be easily adopted to achieve this. Single phase systems are the most commonly studied in this regard, due to the simplicity of their process parameters. These systems involve two or more miscible solvents mixed in a micromixer. The change in polarity, as the solvents mix, promotes nanoprecipitation and the formulation of nanomedicines. This method has been used for the production of a variety of nanomedicines including liposomes (Jahn et al., 2007; Kastner et al., 2015), lipid nanoparticles (Maeki et al., 2017), solid lipid nanoparticles (Anderluzzi and Perrie, 2019; Liu et al., 2013), polymeric nanoparticles (Bally et al., 2012; Roces et al., 2020) and PEGylated liposomes (Dong et al., 2019). To increase output, systems can be scaled-out or scaled-up (Shrimal et al., 2020). Scaling-out through parallelisation can be achieved by placing multiple micromixers in parallel so that the production rate can be directly multiplied with the same properties as those prepared at bench-scale. However, this design requires complex fluid flow distribution, and potentially a separate set of pumps/pressure controls for each fluid inlet. In contrast, scaling-up involves selective dimension enlargement with the microfluidic channel size being increased such that the throughput can be increased. However, to achieve the correct mapping of the physico-chemical nanoparticle attributes, the mixing and nanoprecipitation must be maintained across the micromixers irrespective of channel size (Kirschneck and Tekautz, 2007). A major advantage of the toroidal micromixer outlined is the ability to offer scale-independent production as the systems can be run at small laboratory-scale through to continuous production using the same parameter set points, normal operating range and proven acceptable range via scale-up rather than scale-out. As shown in Figures 2 to 7, the physico-chemical attributes of liposomes produced using the new toroidal mixer map directly to those produced on the staggered herringbone mixer. As an example, the direct mapping of critical process parameters and normal operating ranges for protein-loaded neutral liposomes from the staggered herringbone mixer to the toroidal mixer run at bench-scale are shown in Table 4.

Table 4. Critical process parameter mapping comparison for neutral liposome formulations produced using a staggered herringbone mixer (SHM) and a toroidal mixer (TrM) in terms of particle size (Z-average diameter of 60 ± 10 nm), PDI (< 0.2), zeta potential (-5 to -10 mV), morphology, loading (26 – 36%) and drug release (20 - 30% at 24 h and 70 - 85% at 120 h) (where tested).

		SHM	TrM
Lipid Choice	DSPC	✓	✓
	HSPC	✓	✓
Solvent Choice	EtOH	✓	✓
	MeOH	✓	✓
Flow Rate Ratio	3:1	✓	✓
	5:1	✓	✓
Total Flow Rate	12-20 mL/min	✓	✓
	60 mL/min		✓
	200 mL/min		✓

With this formulation, we set our product specification at: Z-average diameter of 60 ± 10 nm, PDI value of < 0.2, encapsulation efficiency of 26 - 36% and drug release of 20 - 30% at 24 h and 70 - 85% at 120 h. These parameters were selected as markers for reproducibility of the product given each parameter is recognised as a key quality attribute. Furthermore, the new toroidal microfluidic mixer allows the scale-up production of liposomes from 12 mL/min through to 200 mL/min without the need to undertake further process development nor adjustment of other process parameters (summarised in Table 5).

Table 5. Liposomes product specification mapping across three production scales: bench (12mL/min), pre-clinical 60 mL/min) and GMP production (200 mL/min) using the TrM mixer.

Liposome attributes	12 mL/min	60 mL/min	200 mL/min
Particle size: 50 – 70 nm	✓	✓	✓
PDI: < 0.2	✓	✓	✓
Zeta Potential: -5 to – 10 mV	✓	✓	✓
Protein loading: 26 – 36%	✓	✓	✓

When scaling-up microfluidic production, if you want to run a higher flow rate and keep pressure manageable, you need a larger channel. However, with some microfluidic mixer designs, the complexity of their design means there is a practical limit to how large these channels can be made whilst maintaining the desired the fluid flow and nanoprecipitation conditions. With the newly designed planar geometry of the toroidal mixer these issues are circumvented. Furthermore, scalable down-stream processing using tangential flow filtration can be used to support microfluidic production of nanomedicines with a section of examples outlined in Table 3. Whilst in our studies, we use a single column and wash via recirculation, TFF columns can be increased in volume and placed in series to reduce time and improve simplicity (Huter and Strube, 2019). To support in-process monitoring of nanomedicines production, at-line particles sizing can be incorporated as part of a microfluidic production process (Forbes et al., 2019; Roces et al., 2019a) to provide process monitoring and/or product quality control and this could be combined with on-line HPLC methods to consider drug loading. Overall, this manufacturing process allows for the rapid translation of laboratory research to GMP production and provides a direct line of sight from bench to production for nanomedicines.

5. Conclusion

Nanoparticles are well recognised for their ability to improve drug delivery, reducing off-target toxicity and reducing dose requirements. Microfluidics offers new opportunities for the production of nanomedicines, thereby de-risking their application and allowing them to be more widely adopted to improve healthcare outcomes. Both scale-out and scale-up options can be applied to microfluidic production and new developments in microfluidic mixers easily support scale-independent production. This ensures nanoparticles can to be produced with the same critical quality attributes across a range of production speeds and volumes using the same process production parameters, thus providing a direct and rapid production pathway for nanomedicines from bench to commercial product.

Author Contributions: Conceptualization, YP, TL; methodology, CW, NF, CBR, GA, GL, SA, LI, KM, JW, JA, YP; formal analysis, CW, NF, CBR, GL, GA, YP; investigation, CW, NF, CBR, GL, GA, SA, LI, KM, TL, JW, JA, YP; writing, review and editing YP, CW, TL, NF, CBR, GL, GA; visualization, YP, CW, NF, CBR, GL, GA; supervision, YP; project administration and funding acquisition, YP.

Funding: This research was funded by Strathclyde University (CW), EPSRC Centre for Innovative Manufacturing in Emergent Therapies (EPSRC) (EP/I033270/1) (NF), Microsun (NFC-01 Catapult) (CBR) and PHA-ST-TRAIN-VAC (European Commission Project Leveraging Pharmaceutical Sciences and Structural Biology Training to Develop 21st Century Vaccines) (H2020-MSCA-ITN-2015 grant agreement 675370) (Grant agreement ID: 675370) (GL, GA). Collaboration with The University of Nottingham was funded by NanoPrime; an EPSRC and University of Nottingham initiative (EP/R025282/1), TEM instrumentation was supported by the EPSRC (EP/L022494/1) and the University of Nottingham. **Data Access**. All data underpinning this publication is openly available from the University of Strathclyde KnowledgeBase at DOI: https://doi.org/10.15129/91299007-146d-4b44-b1ad-cec8d309612c

References

Akinc, A., Maier, M.A., Manoharan, M., Fitzgerald, K., Jayaraman, M., Barros, S., Ansell, S., Du, X., Hope, M.J., Madden, T.D., Mui, B.L., Semple, S.C., Tam, Y.K., Ciufolini, M., Witzigmann, D., Kulkarni, J.A., van der Meel, R., Cullis, P.R., 2019. The Onpattro story and the clinical translation of nanomedicines containing nucleic acid-based drugs. Nature Nanotechnology 14, 1084-1087.

Allen, T.M., Cullis, P.R., 2013. Liposomal drug delivery systems: from concept to clinical applications. Adv Drug Deliv Rev 65, 36-48.

Anderluzzi, G., Perrie, Y., 2019. Microfluidic Manufacture of Solid Lipid Nanoparticles: A Case Study on Tristearin-Based Systems. Drug Delivery Letters 9, 1-12.

Bally, F., Garg, D.K., Serra, C.A., Hoarau, Y., Anton, N., Brochon, C., Parida, D., Vandamme, T., Hadziioannou, G., 2012. Improved size-tunable preparation of polymeric nanoparticles by microfluidic nanoprecipitation. Polymer 53, 5045-5051.

Barenholz, Y., 2012. Doxil(R)--the first FDA-approved nano-drug: lessons learned. Journal of controlled release : official journal of the Controlled Release Society 160, 117-134.

Belliveau, N.M., Huft, J., Lin, P.J., Chen, S., Leung, A.K., Leaver, T.J., Wild, A.W., Lee, J.B., Taylor, R.J., Tam, Y.K., Hansen, C.L., Cullis, P.R., 2012. Microfluidic Synthesis of Highly Potent Limit-size Lipid Nanoparticles for In Vivo Delivery of siRNA. Mol Ther Nucleic Acids 1, e37.

Bramosanti, M., Chronopoulou, L., Grillo, F., Valletta, A., Palocci, C., 2017. Microfluidic-assisted nanoprecipitation of antiviral-loaded polymeric nanoparticles. Colloids and Surfaces A: Physicochemical and Engineering Aspects 532, 369-376.

Chronopoulou, L., Sparago, C., Palocci, C., 2014. A modular microfluidic platform for the synthesis of biopolymeric nanoparticles entrapping organic actives. Journal of Nanoparticle Research 16.

de Paiva Lacerda, S., Espitalier, F., Hoffart, V., Ré, M.I., 2015. Liquid anti-solvent recrystallization to enhance dissolution of CRS 74, a new antiretroviral drug. Drug Development and Industrial Pharmacy 41, 1910-1920.

Dimov, N., Kastner, E., Hussain, M., Perrie, Y., Szita, N., 2017. Formation and purification of tailored liposomes for drug delivery using a module-based micro continuous-flow system. Scientific Reports 7.

Ding, S., Serra, C.A., Anton, N., Yu, W., Vandamme, T.F., 2019. Production of dry-state ketoprofen-encapsulated PMMA NPs by coupling micromixer-assisted nanoprecipitation and spray drying. Int J Pharm 558, 1-8.

Dobhal, A., Kulkarni, A., Dandekar, P., Jain, R., 2017. A microreactor-based continuous process for controlled synthesis of poly-methyl-methacrylate-methacrylic acid (PMMA) nanoparticles. Journal of Materials Chemistry B 5, 3404-3417.

Dong, Y.-D., Tchung, E., Nowell, C., Kaga, S., Leong, N., Mehta, D., Kaminskas, L.M., Boyd, B.J., 2019. Microfluidic preparation of drug-loaded PEGylated liposomes, and the impact of liposome size on tumour retention and penetration. Journal of Liposome Research 29, 1-9.

EMA, 2018, Onpattro Assessment Report, https://www.ema.europa.eu/en/documents/assessment-report/onpattro-epar-public-assessment-report_.pdf, (Accessed 3 December 2019)

Evers, M.J.W., Kulkarni, J.A., van der Meel, R., Cullis, P.R., Vader, P., Schiffelers, R.M., 2018. State-of-the-Art Design and Rapid-Mixing Production Techniques of Lipid Nanoparticles for Nucleic Acid Delivery. Small Methods 2.

Forbes, N., Hussain, M.T., Briuglia, M.L., Edwards, D.P., Horst, J.H.T., Szita, N., Perrie, Y., 2019. Rapid and scale-independent microfluidic manufacture of liposomes entrapping protein incorporating in-line purification and at-line size monitoring. Int J Pharm 556, 68-81.

Guimaraes Sa Correia, M., Briuglia, M.L., Niosi, F., Lamprou, D.A., 2017. Microfluidic manufacturing of phospholipid nanoparticles: Stability, encapsulation efficacy, and drug release. Int J Pharm 516, 91-99.

Hood, R.R., Vreeland, W.N., DeVoe, D.L., 2014. Microfluidic remote loading for rapid single-step liposomal drug preparation. Lab Chip 14, 3359-3367.

Huter, M.J., Strube, J., 2019. Model-Based Design and Process Optimization of Continuous Single Pass Tangential Flow Filtration Focusing on Continuous Bioprocessing. Processes 7.

Jahn, A., Vreeland, W.N., DeVoe, D.L., Locascio, L.E., Gaitan, M., 2007. Microfluidic Directed Formation of Liposomes of Controlled Size. American Chemical Society 23, 6289-6293.

Jahn, A., Vreeland, W.N., Gaitan, M., Locascio, L.E., 2004. Controlled Vesicle Self-Assembly in Microfluidic Channels with
Hydrodynamic Focusing. Journal of the American Chemical Society 126, 2672-2675.

James, N.D., Coker, R.J., Tomlinson, D., Harris, J.R.W., Gompels, M., Pinching, A.J., Stewart, J.S.W., 1994. Liposomal doxorubicin (Doxil): An effective new treatment for Kaposi's sarcoma in AIDS. Clinical Oncology 6, 294-296.

Joshi, S., Hussain, M.T., Roces, C.B., Anderluzzi, G., Kastner, E., Salmaso, S., Kirby, D.J., Perrie, Y., 2016. Microfluidics based manufacture of liposomes simultaneously entrapping hydrophilic and lipophilic drugs. International Journal of Pharmaceutics 514, 160-168.

Kamholz, A.E., Yager, P., 2001. Theoretical Analysis of Molecular Diffusion in Pressure-Driven Laminar Flow in Microfluidic Channels. Biophysical Journal 80, 155-160.

Kastner, E., Verma, V., Lowry, D., Perrie, Y., 2015. Microfluidic-controlled manufacture of liposomes for the solubilisation of a poorly water soluble drug. Int J Pharm 485, 122-130.

Khadke, S., Roces, C.B., Cameron, A., Devitt, A., Perrie, Y., 2019. Formulation and manufacturing of lymphatic targeting liposomes using microfluidics. Journal of controlled release : official journal of the Controlled Release Society.

Kirschneck, D., Tekautz, G., 2007. Integration of a Microreactor in an Existing Production Plant. Chemical Engineering & Technology 30, 305-308.

Kulkarni, J.A., Tam, Y.Y.C., Chen, S., Zaifman, J., Cullis, P.R., Biswas, S., 2017. Rapid synthesis of lipid nanoparticles containing hydrophobic inorganic nanoparticles. Nanoscale 9.

Le The, H., Le Thanh, H., Dong, T., Ta, B.Q., Tran-Minh, N., Karlsen, F., 2015. An effective passive micromixer with shifted trapezoidal blades using wide Reynolds number range. Chemical Engineering Research and Design 93, 1-11.

Lee, C.-Y., Wang, W.-T., Liu, C.-C., Fu, L.-M., 2016. Passive mixers in microfluidic systems: A review. Chemical Engineering Journal 288, 146-160.

Lin, W.S., Malmstadt, N., 2019. Liposome production and concurrent loading of drug simulants by microfluidic hydrodynamic focusing. Eur Biophys J 48, 549-558.

Liu, D., Herranz-Blanco, B., Mäkilä, E., Arriaga, L.R., Mirza, S., Weitz, D.A., Sandler, N., Salonen, J., Hirvonen, J., Santos, H.A., 2013. Microfluidic Templated Mesoporous Silicon–Solid Lipid Microcomposites for Sustained Drug Delivery. ACS Applied Materials & Interfaces 5, 12127-12134.

Lou, G., Anderluzzi, G., Woods, S., Roberts, C.W., Perrie, Y., 2019. A novel microfluidic-based approach to formulate size-tuneable large unilamellar cationic liposomes: Formulation, cellular uptake and biodistribution investigations. Eur J Pharm Biopharm 143, 51-60.

Maeki, M., Fujishima, Y., Sato, Y., Yasui, T., Kaji, N., Ishida, A., Tani, H., Baba, Y., Harashima, H., Tokeshi, M., 2017. Understanding the formation mechanism of lipid nanoparticles in microfluidic devices with chaotic micromixers. PLoS One 12, e0187962.

Morikawa, Y., Tagami, T., Hoshikawa, A., Ozeki, T., 2018. The Use of an Efficient Microfluidic Mixing System for Generating Stabilized Polymeric Nanoparticles for Controlled Drug Release. Biological and Pharmaceutical Bulletin 41, 899-907.

Obeid, M.A., Khadra, I., Albaloushi, A., Mullin, M., Alyamani, H., Ferro, V.A., 2019. Microfluidic manufacturing of different niosomes nanoparticles for curcumin encapsulation: Physical characteristics, encapsulation efficacy, and drug release. Beilstein J Nanotechnol 10, 1826-1832.

Olson, J.A., Adler-Moore, J.P., Jensen, G.M., Schwartz, J., Dignani, M.C., Proffitt, R.T., 2008. Comparison of the physicochemical, antifungal, and toxic properties of two liposomal amphotericin B products. Antimicrob Agents Chemother 52, 259-268.

Patil, P., Khairnar, G., Naik, J., 2015. Preparation and statistical optimization of Losartan Potassium loaded nanoparticles using Box Behnken factorial design: Microreactor precipitation. Chemical Engineering Research and Design 104, 98-109.

Rivnay, B., Wakim, J., Avery, K., Petrochenko, P., Myung, J.H., Kozak, D., Yoon, S., Landrau, N., Nivorozhkin, A., 2019. Critical process parameters in manufacturing of liposomal formulations of amphotericin B. Int J Pharm 565, 447-457.

Roces, C.B., Christensen, D., Perrie, Y., 2020. Translating the fabrication of protein-loaded poly(lactic-co-glycolic acid) nanoparticles from bench to scale-independent production using microfluidics. Drug Delivery and Translational Research.

Roces, C.B., Hussain, M.T., Schmidt, S.T., Christensen, D., Perrie, Y., 2019a. Investigating Prime-Pull Vaccination through a Combination of Parenteral Vaccination and Intranasal Boosting. Vaccines 8.

Roces, C.B., Khadke, S., Christensen, D., Perrie, Y., 2019b. Scale-Independent Microfluidic Production of Cationic Liposomal Adjuvants and Development of Enhanced Lymphatic Targeting Strategies. Mol Pharm 16, 4372-4386.

Rudyak, V., Minakov, A., 2014. Modeling and Optimization of Y-Type Micromixers. Micromachines 5, 886-912.

Shrimal, P., Jadeja, G., Patel, S., 2020. A review on novel methodologies for drug nanoparticle preparation: Microfluidic approach. Chemical Engineering Research and Design 153, 728-756.

Tóth, E., Holczer, E., Iván, K., Fürjes, P., 2014. Optimized Simulation and Validation of Particle Advection in Asymmetric Staggered Herringbone Type Micromixers. Micromachines 6, 136-150.

Umrethia, M., Kett, V.L., Andrews, G.P., Malcolm, R.K., Woolfson, A.D., 2010. Selection of an analytical method for evaluating bovine serum albumin concentrations in pharmaceutical polymeric formulations. J Pharm Biomed Anal 51, 1175-1179.van Ballegooie, C., Man, A., Andreu, I., Gates, B.D., Yapp, D., 2019. Using a Microfluidics System to Reproducibly Synthesize Protein Nanoparticles: Factors Contributing to Size, Homogeneity, and Stability. Processes 7.

Webb, C., Khadke, S., Schmidt, S.T., Roces, C.B., Forbes, N., Berrie, G., Perrie, Y., 2019. The Impact of Solvent Selection: Strategies to Guide the Manufacturing of Liposomes Using Microfluidics. Pharmaceutics 11.

Yanagi, T., Tachikawa, K., Wilkie-Grantham, R., Hishiki, A., Nagai, K., Toyonaga, E., Chivukula, P., Matsuzawa, S., 2016. Lipid Nanoparticle-mediated siRNA Transfer Against PCTAIRE1/PCTK1/Cdk16 Inhibits In Vivo Cancer Growth. Mol Ther Nucleic Acids 5, e327.

Yeo, L.K., Olusanya, T.O.B., Chaw, C.S., Elkordy, A.A., 2018. Brief Effect of a Small Hydrophobic Drug (Cinnarizine) on the Physicochemical Characterisation of Niosomes Produced by Thin-Film Hydration and Microfluidic Methods. Pharmaceutics 10.

Zhang, X., Chen, H., Qian, F., Cheng, Y., 2018. Preparation of itraconazole nanoparticles by anti-solvent precipitation method using a cascaded microfluidic device and an ultrasonic spray drier. Chemical Engineering Journal 334, 2264-2272.

Zhang, X., Goel, V., Attarwala, H., Sweetser, M.T., Clausen, V.A., Robbie, G.J., 2020. Patisiran Pharmacokinetics, Pharmacodynamics, and Exposure-Response Analyses in the Phase 3 APOLLO Trial in Patients With Hereditary Transthyretin-Mediated (hATTR) Amyloidosis. J Clin Pharmacol 60, 37-49.

Zhigaltsev, I.V., Belliveau, N., Hafez, I., Leung, A.K., Huft, J., Hansen, C., Cullis, P.R., 2012. Bottom-up design and synthesis of limit size lipid nanoparticle systems with aqueous and triglyceride cores using millisecond microfluidic mixing. Langmuir 28, 3633-3640.